JACS
JOURNAL OF THE AMERICAN CHEMICAL SOCIETY

Article

pubs.acs.org/JACS

Improved Biocatalysts from a Synthetic Circular Permutation Library of the Flavin-Dependent Oxidoreductase Old Yellow Enzyme

Ashley B. Daugherty,[†] Sridhar Govindarajan,[‡] and Stefan Lutz*[,†]

[†]Department of Chemistry, Emory University, 1515 Dickey Drive, Atlanta, Georgia 30084, United States
[‡]DNA2.0, 1140A O'Brian Drive, Menlo Park, California 94025, United States

Supporting Information

ABSTRACT: Members of the old yellow enzyme (OYE) family are widely used, effective biocatalysts for the stereoselective trans-hydrogenation of activated alkenes. To further expand their substrate scope and improve catalytic performance, we have applied a protein engineering strategy called circular permutation (CP) to enhance the function of OYE1 from *Saccharomyces pastorianus*. CP can influence a biocatalyst's function by altering protein backbone flexibility and active site accessibility, both critical performance features because the catalytic cycle for OYE1 is thought to involve rate-limiting conformational changes. To explore the impact of CP throughout the OYE1 protein sequence, we implemented a highly efficient approach for cell-free cpOYE library preparation by combining whole-gene synthesis with in vitro transcription/translation. The versatility of such an ex vivo system was further demonstrated by the rapid and reliable functional evaluation of library members under variable environmental conditions with three reference substrates ketoisophorone, cinnamaldehyde, and (*S*)-carvone. Library analysis identified over 70 functional OYE1 variants with several biocatalysts exhibiting over an order of magnitude improved catalytic activity. Although catalytic gains of individual cpOYE library members vary by substrate, the locations of new protein termini in functional variants for all tested substates fall within the same four distinct loop/lid regions near the active site. Our findings demonstrate the importance of these structural elements in enzyme function and support the hypothesis of conformational flexibility as a limiting factor for catalysis in wild type OYE.

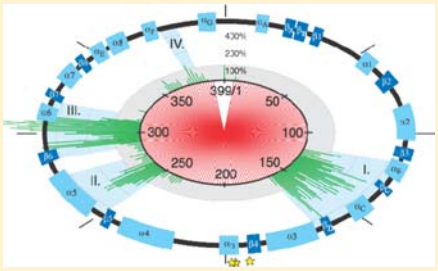

INTRODUCTION

The reduction of alkenes is a widely used and effective strategy for the asymmetric synthesis of chiral building blocks. While traditional catalysts for these reactions include chiral transition metal complexes[1−3] and organocatalysts,[4] enzymes offer a highly selective, evolvable, and sustainable alternative.[5−7] More specifically, ene-reductases of the old yellow enzyme (OYE) family [EC 1.3.1.31] are known to catalyze the highly stereoselective trans-hydrogenation of α,β-unsaturated aldehydes, ketones, carboxylates, nitriles, and nitroalkenes.[8−14] The redox chemistry of OYEs is facilitated by a noncovalently bound flavin mononucleotide (FMN) cofactor. Following reduction of the alkene substrate, the FMN is regenerated via hydride transfer from NADPH (Scheme 1).

The popularity of OYEs in biotechnological and pharmaceutical applications has resulted in the isolation and characterization of family members from a variety of organisms, providing a rich source of oxidoreductases for the conversion of alkenes.[10,12,13,15−19] At the same time, these biocatalysts represent attractive targets for protein engineers to further improve and customize their functional performance. A number of structure-guided site-directed and site-saturation mutagenesis studies, as well as directed evolution experiments, have yielded OYE variants with improved catalytic properties including enhanced turnover rates, reversed enantioselectivity, and increased stability.[20−25] Unfortunately, the reported gains in catalytic activity were generally modest (2- to 4-fold). However, potential benefits of amino acid substitution in OYE family members are possible as demonstrated by the complete reversal of enantioselectivity as a result of a single amino acid change.[23] A review of past OYE engineering studies also identified a major experimental challenge. Following standard heterologous expression of OYEs in *Escherichia coli* (*E. coli*), the functional characterization of the exogenous oxidoreductase is complicated by the host's endogenous reductase activity, hence requiring additional purification steps prior to functional evaluation.[20] Consequently, library analysis has typically been limited to either small numbers of variants or to substrates with low background from host reductases.[22,23] Future efforts involving larger, more comprehensive protein libraries for tailoring OYE family members would clearly benefit from a more effective library preparation and analysis protocol.

Our OYE engineering efforts were motivated by a number of biochemical studies and crystallographic structure analyses that suggested substantial conformational changes as part of the enzyme's catalytic cycle. Spectroscopic evidence for such conformational changes in kinetic measurements and structural differences in crystals of apo-form and substrate-bound OYEs as well as more recent data from an engineering study of *Zymomonas mobiliz* NCR enoate reductase all support the hypothesis that structural rearrangements of loops and domains

Received: July 24, 2013
Published: August 29, 2013

   dx.doi.org/10.1021/ja4074886 | *J. Am. Chem. Soc.* 2013, 135, 14425−14432

Scheme 1

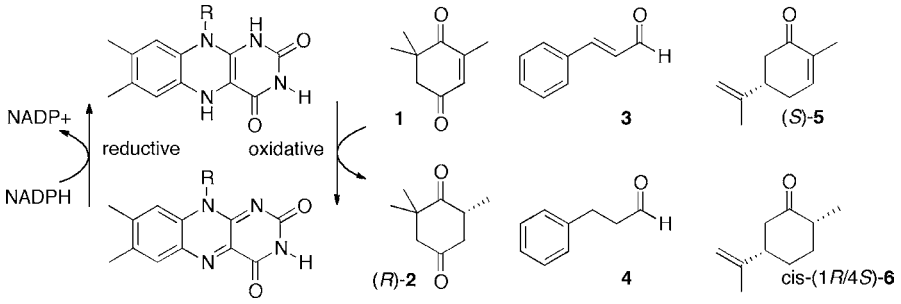

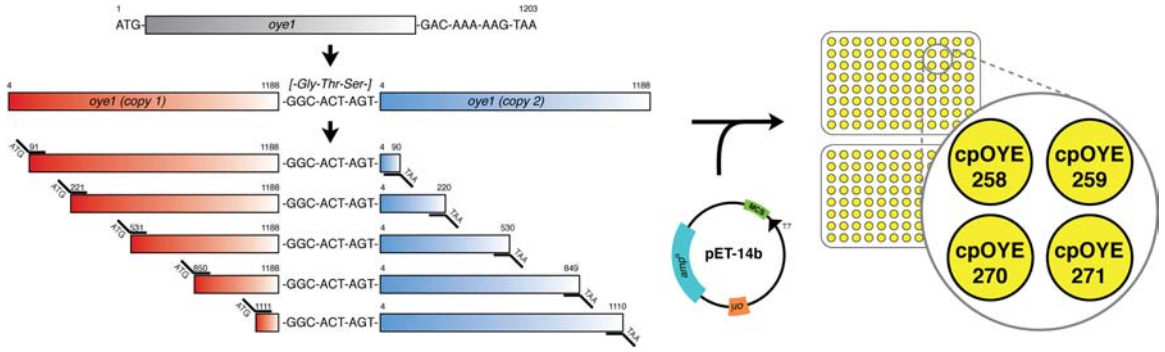

Figure 1. Assembly of cpOYE library via whole-gene synthesis. Two copies of truncated *oye1* (marked in red and blue) were prepared that lack the three native C-terminal amino acids and the Start/Stop codons. The two genes were assembled in tandem and connected by a nine-nucleotide sequence encoding the -Gly-Thr-Ser- linker. PCR amplification with site-specific primers and the tandem repeat as template yielded individual members of the CP library and reintroduced Start/Stop codons, as well as flanking restriction sites for the subsequent cloning into pET-14b. Correct gene constructs (cpOYE*n*) were confirmed by DNA sequencing, sorted, and stored as purified plasmids in microtiterplates.

play an important and possibly rate-limiting role in the catalytic function of these enzymes.[25−31] We therefore decided to test the functional role of various flexible regions in OYE1 from *Saccharomyces pastorianus* (formerly *S. carlsbergensis*), the most extensively studied member of the OYE family, by a protein engineering strategy called circular permutation (CP). During CP, a protein's original amino and carboxyl termini are covalently linked by a peptide linker and new termini are introduced elsewhere in the protein structure through the breakage of a peptide bond.[32] While such termini relocation leaves the amino acid composition of the protein unchanged, the sequence reorganization has been shown to affect a protein's local conformational flexibility. For new termini positioned near an enzyme active site, the altered protein dynamics can significantly impact catalytic performance by translating into greater active site accessibility and modifying rate-determining structural changes.[33−38]

Here, we report on the identification and characterization of catalytically improved OYE1 variants via CP. To address the aforementioned practical limitations for working with combinatorial libraries of OYE, we have opted for a whole-gene synthesis approach that gives access to an idealized gene library with maximal (theoretical) diversity at minimal size. Subsequent synthesis of the corresponding cpOYE variants is accomplished via in vitro transcription/translation (IVTT) using the chemically defined PURE system that almost completely eliminates background reductase activity.[39,40] This ex vivo protein engineering strategy has proved highly effective for the parallel synthesis of hundreds of OYE library members whose catalytic activity can be assessed without further need for purification. The evaluation of our new protocol for OYE1 library screening on three reference substrates is described. The approach has helped to identify a number of candidates with significantly (>10-fold) enhanced catalytic performance. Evidence in support of the critical role of loop and domains near the active site is found in the systematic analysis of protein variants with multiple substrates and detailed characterization of selected cpOYE variants.

MATERIAL AND METHODS

Materials. Whole-gene synthesis was performed by DNA2.0 (Menlo Park, CA). PURExpress kits were purchased from New England Biolabs (Ipswich, MA). All reagents, substrates, and reference materials were obtained from Sigma-Aldrich (St. Louis, MO) unless otherwise indicated.

cpOYE1 Library Synthesis. The gene encoding OYE1 from *S. pastorianus* (formerly *S. carlsbergensis*; NCBI access number X53597.1) served as starting sequence for our experiments. The CP library was prepared by PCR amplification of gene sequences encoding the individual variants using an *oye1* tandem repeat as template (Figure 1). The tandem repeat was created by whole-gene synthesis, linking two copies of *oye1* head-to-tail via an oligonucleotide sequence encoding a three amino acid linker (-Gly-Ser-Thr-). The Start and Stop codons of the 399 amino acid enzyme were eliminated in the tandem repeat. Subsequently, gene sequences corresponding to individual circular permuted enzymes were obtained by PCR amplification using the tandem repeat as template in combination with sequence-specific oligonucleotide primers. In the 5′-regions of the forward primers, a ATG start codon was included while reverse primers carried a TAA termination codon. The PCR products were subcloned into pET-14b (Novagen) via flanking type IIs restriction endonuclease cleavage sites (*Bsa*I) to enable ligation of PCR products into the vector's *Nco*I/*Xho*I sites independent of variations in the *oye1* library sequences. Following transformation of individual ligation reactions into *E. coli*, plasmid DNA from selected colonies was extracted and gene sequences were verified by DNA sequencing. Aliquots of confirmed plasmids carrying

dx.doi.org/10.1021/ja4074886 | J. Am. Chem. Soc. 2013, 135, 14425−14432

specific library members were stored separately in 96-well microtiter plates.

Primary Library Screening. All members of the cpOYE library were initially evaluated for catalytic function by IVTT followed by an in situ ene-reductase activity assay. Overall, the IVTT reactions were assembled using the PURExpress in vitro protein synthesis kit (PURE) following the manufacturer's protocol with a few adjustments (see below) optimized for our application. Reactions were assembled in a 96-well microtiter plate on a 10 μL scale containing PURExpress solution A, PURExpress solution B, 100 μM FMN, 10 units of RNase inhibitor (NEB), 100 ng of DNA template, and nuclease-free H_2O. All reactions from the cpOYE library screening were run simultaneously with wild type OYE1 (positive control) and dihydrofolate reductase (DHFR, negative control, provided with the PURExpress kit) under the same experimental conditions. The mixtures were incubated at 37 °C for 2.5 h to allow for adequate protein synthesis prior to the activity assay. The mixtures were cooled to 4 °C to stop the reaction. Subsequently, ene-reductase activity was assessed under anaerobic conditions (Coy Laboratory Products, Grass Lake, MI) at ambient temperature utilizing glucose dehydrogenase (GDH) from *Thermoplasma acidophilum* for NADPH regeneration. The IVTT reaction was mixed with substrate (200 μM ketoisophorone (**1**), 200 μM cinnamaldehyde (**3**), or 1 mM *S*-carvone (**5**)), 200 μM $NADP^+$, 2 U of GDH, and 100 mM glucose. The 30 μL assay ran for 2.5 h (because of high turnover, reaction time for **3** was reduced to 30 min) and was quenched by mixing with an equal amount of ethyl acetate containing 1 mM cyclohexanone as internal standard. A sample of the organic phase was injected on an Agilent Technologies 6850 GC machine equipped with a chiral CycloSil-B column (30 m × 0,32 mm/0.25 μm, Agilent, Santa Clara, CA) using hydrogen as the carrier gas (flow rate 1.8 mL/min) and an FID detector (detector temperature 200 °C, split ratio 25:1). The temperature program for **1**−**4** was the following: 150 °C, hold 10 min (retention time for **1** = 3.54 min, **2** = 3.86 min ((*R*)-isomer), 3.95 min ((*S*)-isomer), **3** = 6.1 min, **4** = 3.64 min. For **5** and **6**, it was the following: 90 °C, hold 5 min, then 1 °C/min to 120 °C (retention time for **5** = 27.54 min, **6** = 23.1 min ((1*R*/4*S*)-isomer), 22.92 min ((1*S*/4*S*)-isomer). The percent conversions and enantiomeric excess were calculated from substrate and product integration areas and were quantified using standard curves generated using known amounts of the substrate and product.

Protein Expression and Purification. Selected members of the cpOYE library were chosen for a more detailed in vitro characterization in order to confirm and further characterize interesting variants from the primary library screening analysis. Individual plasmid DNA encoding the corresponding library members was initially transformed in *E. coli* BL21(DE3)pLysS for expression. Colonies were cultured in 2 mL of LB medium containing chloramphenicol (34 μg/mL) and ampicillin (100 μg/mL) overnight at 37 °C. The overnight culture was used to inoculate 2YT medium containing the same antibiotics, and cultures were grown at 37 °C until the OD(600) reached 0.5−0.7. Overexpression was induced by addition of IPTG to a final concentration of 0.4 mM, and cultures were overexpressed for 18 h at 20 °C. Subsequently, cultures were centrifuged for 20 min at 4 °C and 4000*g* and cell pellets were stored at −20 °C until purification. The purification of wild type OYE1 and variants followed the same purification procedure. Cell pellets from a 250 mL culture were resuspended in 6 mL of buffer A (40 mM Tris-HCl (pH 8.0), 20 mM NaCl). To the mixture, 75 μL of protease inhibitor cocktail (Sigma), 7.5 μL of benzonase (Novagen), and 10 μM PMSF were added and stored on ice for 30 min. Cells were lyzed using sonication (8× with 10 s pulses and 20 s pauses). After centrifugation for 30 min at 4 °C and 10000*g*, the clear lysate was further purified via anion-exchange chromatography (HiTrap Q HP 5 mL column pre-equilibrated with buffer A). The column was washed with 2 column volumes (CV) of buffer A, followed by a linear gradient to 100% buffer B (40 mM Tris-HCl (pH 8.0), 1 M NaCl) over 10 CV. Product fractions were combined and concentrated to ∼1 mL using a Millipore filter unit (MWCO, 10 kDa). In a final polishing step, proteins were purified by size exclusion chromatography (Superdex 200, 10/300 GL column equilibrated with buffer C (40 mM Tris-HCl (pH 8.0), 300 mM NaCl); flow rate, 0.5 mL/min). Elution of protein was monitored by UV detection at 280 and 460 nm, and product fractions were combined. SDS−PAGE analysis of the final product showed >95% purity.

Spectral Properties of OYE1 Variants. All spectral analysis of OYE1 and permutants was completed using a Varian Cary 100 spectrophotometer. The extinction coefficient for each variant was determined by recording the absorbance spectrum of the protein-bound FMN solution in 10 mM Tris-HCl (pH 7.5) buffer. A 25 μL aliquot of 10% SDS was added to denature the protein, and spectra were recorded until changes were no longer observed. The extinction coefficient for each enzyme-bound FMN was calculated using the following equation: $\varepsilon = (\varepsilon_{\text{free(FMN)}}, 12\,500\ M^{-1}\ cm^{-1}) \times$ (absorbance at λ_{max} of FMN_{bound} prior to SDS treatment)/(absorbance at λ_{max} of FMN_{bound} after SDS).[41]

Phenolate inhibitor binding assays were completed at room temperature in 100 mM potassium phosphate buffer, pH 7, using a cuvette with a 1 cm path length (Figure S1) The initial enzyme concentration (10−30 μM) in each experiment was calculated by the corresponding FMN extinction coefficient. Aliquots of *p*-hydroxybenzaldehyde were added to the protein solution, and spectra were recorded after 3 min of equilibration until apparent saturation was reached. The long wavelength charge transfer maximum values for each data set were determined by first derivative analysis, and extinction coefficients were calculated based on the absorbance values (Table 2). Separately, dissociation constants were calculated by plotting $[\text{ligand}]_{free}$ versus Y (fractional saturation of OYE) and analysis by nonlinear curve fit using GraphPad Prism 6 (GraphPad, La Jolla, CA) (Figure S1 inserts).

Activity Assays. The enzyme concentration for each cpOYE variant was determined based on the extinction coefficient of protein-bound FMN. Purified enzyme was assayed in an anaerobic chamber (Coy LabProducts) by incubating 0.1−1 μM enzyme with 1 mM **1**, 200 μM $NADP^+$, 5 U of GDH, and 100 mM glucose in 500 μL total reaction volume. The reaction was monitored over 45 min (timed to achieve less than 30% product formation) by taking aliquots and mixing with an equal amount of ethyl acetate and analyzed via GC (see above). The product was quantified using a standard curve generated using known amounts of the product (*R*)-levodione (**2**) and 1 mM cyclohexanone as internal standard. Alternatively, turnover was monitored spectrophotometrically at ambient temperatures with the Bioteck EPOCH plate reader housed in the anaerobic chamber. Purified enzyme was assayed following the decrease in absorbance of NADPH at 340 nm (molar extinction coefficient of 6220 $M^{-1}\ cm^{-1}$). The 300 μL mixture contained 100 mM sodium phosphate buffer (pH 7.0), 1 mM appropriate substrate (from 20 mM stock in ethanol), 100 μM NADPH, and 0.1−1 μM enzyme. For **3**, where substrate saturation was not a problem, kinetics constants were determined by fitting initial rates to the Michaelis−Menten equation through a nonlinear curve fit using Origin7 (OriginLab, Northampton, MA) (Table S1). The stereoselectivity displayed by the permutants for reducing (*S*)-**5** was determined by incubating 25 μg of enzyme with 5 mM substrate, 200 μM $NADP^+$, 5 U of GDH, and 100 mM glucose in 500 μL total reaction volume. The reaction was carried out for 24 h at room temperature. After the reaction was quenched, the aqueous portion was extracted with an equal amount of ethyl acetate and the organic layer analyzed by chiral GC.

Stopped Flow Experiments. Measurements were made on an OLIS RSM-1000 (Olis Inc., Bogart, GA) stopped flow spectrophotometer under anaerobic conditions in 50 mM Tris-HCl (pH 7.5) at 25 °C. For the reductive half reaction, OYE1 or cpOYE303 (10 μM) was mixed in the spectrophotometer with NADPH (final concentration, 50−500 μM). The oxidative half reaction was studied with **1** as substrate. Enzyme (13 μM) was preincubated with 20 μM NADPH to completely reduce FMN, followed by mixing with **1** (0.25 and 0.5 mM for OYE1; 0.5 and 1 mM for cpOYE303). Spectra were recorded with delays of 10 and 100 s after mixing. All data analysis was performed in GraphPad Prism 6 (GraphPad, La Jolla, CA).

RESULTS AND DISCUSSION

The structurally and functionally well-characterized OYE1 from *S. pastorianus* was chosen to test our hypothesis that CP of an OYE family member could yield variants with improved catalytic performance. Initially, we analyzed representative structures of OYE1 (PDB access codes 1OYA[30] and 1K03[26]) to determine a suitable linker sequence for connecting the native amino and carboxyl termini. Trimming the C-terminus by three residues shortened the termini distance from 13 to 6 Å without impacting the catalytic performance of the wild type enzyme. The remaining (shorter) gap was bridged by a flexible, hydrophilic three-amino acid residue linker (-Gly-Thr-Ser-).

Taking advantage of whole-gene synthesis, we abandoned the previously employed random circular permutation protocol[33,42] to instead prepare a fully synthetic DNA library of circular permuted OYE1 (cpOYE) variants. A tandem-OYE1 gene sequence was prepared by chemical DNA synthesis that served as template for PCR amplification of individual cpOYE variants (Figure 1). This strategy dramatically reduces the size of the circular permutation library by eliminating out-of-frame and inversely cloned representatives in the sequence pool. Furthermore, parallel cloning of individual genes into an appropriate DNA vector for protein expression followed by verification of the correct DNA sequence for each library member creates a chemically defined collection of enzyme variants. Such up-front effort during library generation is advantageous, as it dramatically simplifies library analysis by eliminating the need for oversampling. For practical reasons, we created a focused cpOYE library by synthesizing only every other possible variant, starting with even-numbered positions at the N-terminus of OYE1. In addition, variants within ±6 amino acids to the native termini were left out, as they are predicted to at best show wild type-like activity. Following the initial functional evaluation of this primary library, odd-numbered variants in regions of interest were quickly prepared by the same PCR-based method. Over the course of this entire study, we synthesized and screened a total of 228 cpOYE variants, identifying roughly 70 members (~30%) in our circular permutation library with equal or better than wild type activity for reduction of ketoisophorone (**1**), a widely used reference substrate for the functional evaluation of OYE family members (see below).

Building on the idea of a synthetic protein engineering approach, we employed the PURE system for functional analysis of the cpOYE library. PURE distinguishes itself from other IVTT systems in that all of its components are isolated and purified individually, followed by reconstitution of a chemically fully defined functional protein synthesis machinery.[39,40] As such, PURE dramatically lowers the background signal caused by contaminating endogenous reductases in cell-based in vitro and in vivo expression systems and allows for direct assaying of enzyme activity (Figure S2). Furthermore, PURE is highly scalable and allows for parallel synthesis of library members in 96-well microtiter plate format with relatively consistent protein yields (±50% based on SDS–PAGE analysis; data not shown). In subsequent activity assays, a 10 μL PURE reaction produced enough enzyme (~ 0.1 μM) for detecting reduction of **1** by OYE1 variants with as little as 10% of wild type activity. Activity assays performed under anaerobic conditions maximize the signal-to-noise ratio, presumably eliminating side reactions and enzyme inactivation by reactive oxygen species generated in the presence of reduced FMN.[20] Finally, expression of catalytically competent OYE required supplementation of the IVTT reaction mixture with FMN. Maximum enzyme activity was reached at [FMN] > 1 μM, which is approximately 100-fold above the reported dissociation constant for FMN in OYE1 (Figure S3).[43] We further raised the [FMN] to 100 μM to ensure saturation of enzyme with cofactor, even for engineered OYEs with potentially lower cofactor binding affinity.

Our initial functional evaluation of the cpOYE library focused on the stereoselective reduction of **1** to (*R*)-**2**, one of the most prominent industrial application for ene-reductases and a widely used standard for the functional evaluation of OYE family members.[16,17,44−47] Preliminary screening with PURE quickly identified ~70 cpOYE variants with catalytic activity equal to or better than wild type enzyme. The location of the new termini in these active variants fell into four distinct sectors within the primary sequence (Figure 2A). Sector I covers most of the exterior helical subdomain (amino acid residues 125−160, numbering based on OYE1), while sectors II and III include loop/helix regions 5 (residues 250−265) and 6 (residues 290−310), respectively (Figure 3). Sector IV represents a short loop (residues 375−380) near the native C-terminus. The activity assay suggested that permutants with new termini in sector III were particularly beneficial for effective reduction of **1**, showing >400% of wild type activity for multiple cpOYE variants. Analysis of the reaction mixtures by chiral GC confirmed unchanged (*R*)-enantioselectivity for all active cpOYE variants with native-like ee_R-values of >98%. From a practical perspective, we were interested in whether the observed activity differences in PURE were reliable predictors of catalytic activity measured with purified enzyme. To assess the predictability of activity in PURE, we selected nine cpOYE variants (cpOYEs 146, 154, 160, 257, 260, 291, 303, 306, and 378; the number indicates the location of a variant's new N-terminal based on the numbering of residues in wild type enzyme) which showed 1- to 4-fold activity gains over OYE1 in the PURE reactions with **1**. Enzyme samples of these nine CP variants and OYE1 were obtained through (traditional) heterologous expression and purification, followed by kinetics measurements of individual conversion rates for **1** (Table 1). Determination of the Michaelis−Menten parameters was not possible, as enzyme saturation could not be reached because of limited solubility of **1**. The kinetics data showed that the rate increases by up to 19-fold (for cpOYE303) over wild type enzyme. The data also indicate that PURE systematically underestimates the rates compared to purified enzyme. Nevertheless, the observed changes in the IVTT system were overall proportional; the top performers in the PURE system also showed the highest catalytic gains with purified enzyme. These results suggest that the IVTT data is semiquantitative and can be used as reliable predictor of enzyme activity.

The experimental data for reduction of **1** led to three questions concerning the structure−function relationship in these engineered OYE variants: (a) Will the same four sectors be identified upon screening with other substrates? (b) Will sector III always be the preferred site for termini relocation? (c) Will native (*R*)-enantioselectivity be preserved for other substrates? We explored the first question by screening the cpOYE library for improvements in ene-reductase activity with cinnamaldehyde (**3**) and (*S*)-carvone (**5**) as substrates (Figure 2B,C). Both compounds are important intermediates in the fragrance and flavor industry. Library screening with these two substrates identified functional variants in the same four sectors

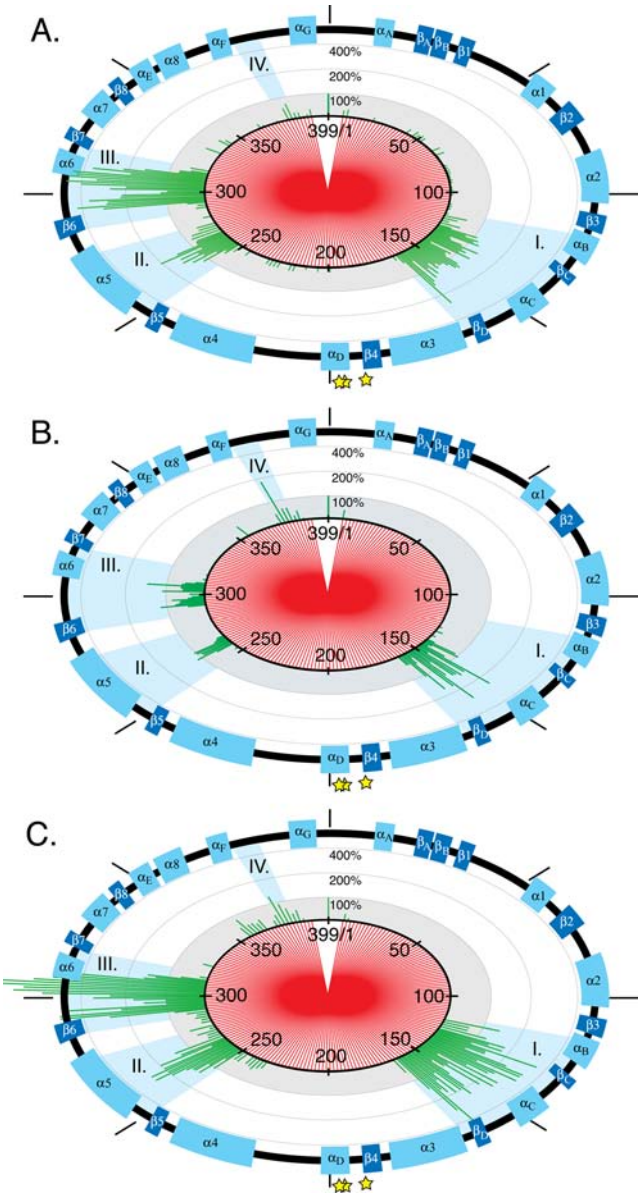

Figure 2. Primary screening data of cpOYE library for ene-reductase activity on (A) ketoisophorone (**1**) to levodione ((*R*)-**2**), (B) cinnamaldehyde (**3**) to dihydrocinnamaldehyde (**4**), and (C) carvone ((*S*)-**5**) to dihydrocarvone (*cis*-(1*R*,4*S*)-**6**). Whole-gene synthesis created a native cpOYE library with perfect distribution (red lines in inner circle). Catalytic activity of library members for each substrate was measured by semiquantitative assay and is reflected in the length of the green lines. Wild-type activity is indicated by the gray-shaded area. The outermost circle marks the secondary structure elements (shades of blue) and active site residues (yellow stars) of OYE1 (399 amino acid residues). For all three substrates, four sectors (I–IV) in the protein sequence with activity equal to or better than that of wild type were identified.

of the protein sequence. For conversion of **3**, the catalytic improvements upon CP appeared moderate, an observation that was confirmed in activity assays with purified enzyme which detected up to 2-fold rate increases in catalytic efficiency for cpOYE260 (Table 1). We hypothesize that the already high catalytic efficiency of OYE1 for reduction of **3** makes it more likely for additional functional gains to be countered by undesirable structural perturbations upon CP. In contrast, the screening of our cpOYE library with **5** showed significant

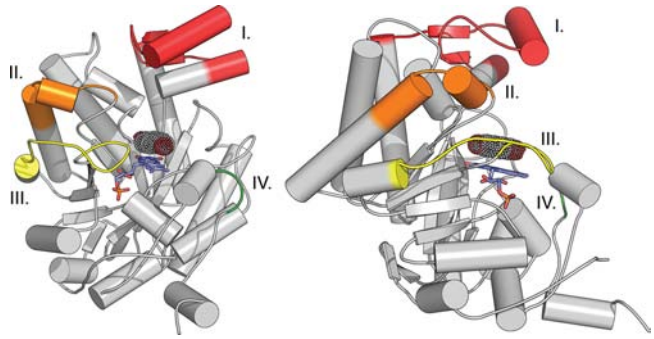

Figure 3. Schematic of OYE1 structure (based on PDB access code 1K03[26]). The FMN cofactor is shown in blue sticks, while the substrate-binding site is occupied by *p*-hydroxybenzaldehyde (dotted cloud). The location of permutation sites that resulted in catalytic improvements are highlighted in red (sectors I), orange (sectors II), yellow (sectors III), and green (sectors IV).

Table 1. Comparison of Biocatalytic Rates for Reduction of Ketoisophorone (1), Cinnamaldehyde (3), and (*S*)-Carvone (5)[a]

variant	IVTT(**1**)[b]	EA(**1**)[c] (min^{-1})	EA(**3**)[d] (min^{-1})	EA(**5**)[d] (min^{-1})
OYE1	1×	6.5 (1×)	53 (1×)	1.9 (1×)
cpOYE146	1.3×	19 (3×)	60 (1.1×)	1.4 (0.8×)
cpOYE154	0.8×	12.2 (2×)	83 (1.5×)	6 (3×)
cpOYE160	1.6×	10.1 (1.6×)	85 (1.6)	9.5 (5×)
cpOYE257	1×	13 (2×)	44 (0.8×)	5.7 (3×)
cpOYE260	2×	25.4 (4×)	113 (2×)	7.7 (4×)
cpOYE291	3.2×	36 (6×)	21 (0.4×)	3.4 (1.8×)
cpOYE303	5.3×	122 (19×)	24 (0.4×)	22.5 (12×)
cpOYE306	4.2×	47.2 (7×)	42 (0.8×)	23.6 (13×)
cpOYE378	0.7×	nd	57 (1×)	5.9 (3×)

[a]Standard error for IVTT data, ±100%; EA data, ±10%. nd = not determined. [b]Fold activity change in based on GC analysis. [c]Conversion rate (fold-change) of regular enzyme activity (EA) measurements via GC. [d]Conversion rate (fold-change) of regular enzyme activity (EA) measurements via UV analysis.

catalytic improvements for variants in all four sectors. These functional gains were independently verified in subsequent activity assays with purified enzyme, showing 3- to 13-fold increases in the rate of conversion (Table 1). As for **1**, the limited substrate solubility of **5** prevents the determination of detailed kinetics parameters, and no changes in the native enzyme's (*R*)-selectivity for the conversion of (*S*)-**5** to *cis*-(1*R*/4*S*)-**6** were detected. In a summary of the screening results for **1**, **3**, and **5**, all active candidates among the OYE1 variants had their new protein termini located in the same four sectors. The exclusivity of functional variants in these sectors might at least in part be associated with protein foldability upon termini relocation. Nevertheless, their proximity to the active site and in some cases significant improvement in catalytic activity over the native enzyme suggest additional benefits arising from changes in conformational flexibility and active site accessibility. The same data also showed that relative catalytic performance of cpOYE variants differs with individual substrates. Although variants in sector III are clearly the best biocatalysts for **1**, sectors I and IV offer slight activity gains for **3** while variants from all four sectors show substantive functional benefits for reduction of **5**. The observed preference of the three substrates for protein termini in certain sectors and those sectors' location

dx.doi.org/10.1021/ja4074886 | J. Am. Chem. Soc. 2013, 135, 14425−14432

Table 2. Spectral Property Changes upon Inhibitor Binding[a]

variant	K_D (μM)[b]	λ_{max} (CT, nm) (ε (M^{-1} cm^{-1}))	λ_{max} (FMN, nm) (ε (M^{-1} cm^{-1}))	$E^{\circ\prime}$ (mV)[c]
OYE1	1.6 ± 0.4	578 (4335)	460 (10600)	−207
cpOYE154	1.0 ± 0.3	582 (3753)	457 (12784)	−196
cpOYE160	0.6 ± 0.2	572 (2971)	462 (11913)	−210
cpOYE257	1.9 ± 0.7	566 (2485)	463 (11341)	−214
cpOYE260	1.1 ± 0.4	580 (2973)	460 (11979)	−200
cpOYE291	4.0 ± 1.0	564 (2956)	464 (12260)	−216
cpOYE303	1.9 ± 0.2	569 (2685)	463 (13147)	−212
cpOYE306	2.9 ± 0.9	565 (2756)	458 (10774)	−215
cpOYE378	2.3 ± 0.9	578 (3702)	458 (12224)	−207

[a]Standard error: ± 5 mV. [b]Dissociation constant for *p*-hydroxybenzaldehyde. [c]$E^{\circ\prime}$ values were estimated based on correlation of λ_{max}(CT) band with FMN $E^{\circ\prime}$ values.[43]

relative to the substrate binding site could provide clues to the underlying structure−function relationship. Future in-depth structure studies on selected cpOYE variants via X-ray crystallography will help to address these questions in more detail. In summary, the relocation of protein termini in OYE1 introduced structural and conformational changes in distinct portions of the active site, in turn affecting substrate binding affinity, orientation, and catalytic turnover.

To further investigate the nature of the catalytic rate enhancements, we conducted a series of rapid reaction kinetics experiments with wild type OYE1 and cpOYE303, the variant with the most significant functional improvements (Figure 4). The enzyme's catalytic cycle can be split into two steps: a reductive half reaction representing the NADPH-driven reduction of the oxidized flavoprotein and an oxidative half reaction involving reoxidation of the reduced flavin cofactor upon substrate conversion (Scheme 1). On the basis of studies by Massey and co-workers, the reductive half reaction can be further divided into three substeps: (i) initial binding of NADPH to enzyme (E)·FMN_{ox} followed by (ii) conformational changes and repositioning of the nicotinamide cofactor from E·FMN_{ox}·NADPH to E*·FMN_{ox}·NADPH, and finally (iii) hydride transfer.[29] For wild type OYE1, formation of E·FMN_{ox}·NADPH is observed in stopped-flow experiments because the adduct generates a short-lived charge-transfer complex with a characteristic red-shifted FMN absorption peak near 460 nm. Subsequent reorientation of the flavin (E*·FMN_{ox}·NADPH) and reduction of the flavin cofactor result in the disappearance of the 460 nm band. In agreement with Massey's data, we detected the intermediate in our reaction catalyzed by wild type OYE1, and yet the global fit analysis of spectral data for the engineered variant cpOYE303 did not indicate accumulation of an observable charge-transfer complex prior to reduction (Figure 4B). At the same time, the overall rates of the reductive half reaction for OYE1 (k_{red} = 5.1 ± 0.2 s^{-1}) and cpOYE303 (k_{red} = 5.4 ± 0.2 s^{-1}) remained largely unchanged (Figure 4C). Given these observations, we rationalized the absence of an intermediate in cpOYE303 with an increased dissociation rate for NADPH from E·FMN_{ox}·NADPH. Such an explanation is also consistent with previous reports from structural studies that emphasized the importance of conformational changes in loop region 5 (amino acid positions 290−310) as part of the reductive half reaction.[31] The location of the new protein termini in cpOYE303 in this region is likely responsible for the lower NADPH binding affinity, reflecting the increased local conformational flexibility upon cleavage of the polypeptide sequence which has been observed in numerous structure studies with circularly permutated proteins.[35,48−51] In summary, protein sequence reorganization by CP does impact the NADPH binding step of the reductive half reaction but at least in the case of cpOYE303 leaves the overall rate of the reductive half reaction unchanged.

In contrast, the observed rate for the oxidative half reaction increases significantly upon CP and largely accounts for the gains in catalytic activity measured by steady-state kinetics. Following preincubation of the two OYEs with NADPH to fully reduce the enzyme-bound FMN, the rates of cofactor reoxidation (k_{ox}) were measured after mixing with **1** (Figure 4D). For both enzymes, the data could be fitted to a single-exponential function, yielding initial rates of conversion for cpOYE303 and OYE1 of 0.63 ± 0.09 s^{-1} and 0.06 ± 0.01 s^{-1}, respectively. The data indicate that FMN reoxidation with **1** is significantly slower than cofactor reduction in both OYEs and likely represents the rate-limiting step in the reaction cycle. More importantly, we observe an 11-fold rate increase for cpOYE303 over OYE1 which accounts for most of the gains in catalytic activity observed for the OYE variant in our steady-state kinetic measurements (Table 1). Although these initial studies do not reveal detailed information regarding the effects of CP on the individual steps along the reaction coordinate, the results clearly show that rate enhancement in the OYE-catalyzed reduction of **1** by cpOYE303 is due to changes in the oxidative half reaction. However, it seems unlikely that the observed functional effect is general. Previous studies have shown that the nature of the rate-limiting step in OYE can change as a function of substrate.[28,29] While we believe that the catalytic gains measured for the reduction of (*S*)-**5** originate from similar beneficial effects on the oxidative half reaction, the lack of change for **3** could be explained by differences in the rate-determining step.

In the absence of detailed crystallographic information, we investigated perturbations of the active site environment as a result of CP via changes in the spectral properties of the flavin cofactor. Upon binding of *p*-hydroxybenzaldehyde to OYE1, Massey and co-workers observed distinct long wavelength charge-transfer bands ranging from 560 to 590 nm with λ_{max} values depending on hydrogen-bonding interactions of the phenolate and the FMN redox potential.[43,52] The spectral properties of cpOYE variants can therefore serve as sensitive probes for the active site environment. Our analysis of representative variants from all four sectors with *p*-hydroxybenzaldehyde did indicate subtle but significant active site changes (Table 2 and Figure S1). While small 2-fold differences in dissociation constants for the phenolate are consistent with overall integrity of the active site binding pocket, the shifts in λ_{max} values of the charge-transfer bands from 564 to 582 nm

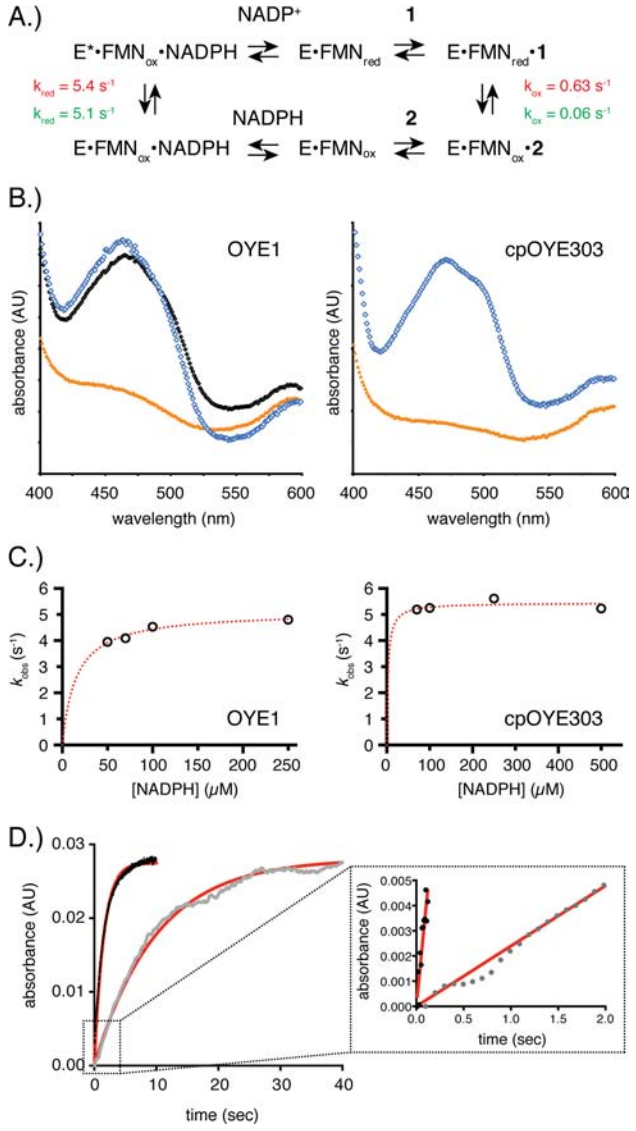

Figure 4. Rapid reaction kinetics for wild type OYE1 and cpOYE303. (A) Complete reaction cycle for OYE with rate constants for the reductive and oxidative half reactions of OYE1 (green) and cpOYE303 (red). (B) Changes in flavin spectra for wild type and cp variant during reductive half reaction. The characteristic absorption band of FMN_{ox} near 460 nm (blue diamonds) disappears upon conversion to FMN_{red} (orange circles). For OYE1, global fit analysis indicates formation of a short-lived intermediate with a slightly red-shifted maximum near 460 nm (black squares) corresponding to the charge-transfer complex in E·FMN_{ox}·NADPH. For cpOYE303, no such intermediate was detectable. (C) Observed rate for the reductive half reaction as a function of [NADPH] based on the disappearance of the FMN_{ox} absorption band. Given experimental restraints to [NADPH] > 50 μM, data analysis was limited to determination of maximum rates (k_{red}). (D) Flavin reoxidation (k_{ox}) upon rapid mixing of E·FMN_{red} with **1** (0.5 mM) under anaerobic conditions followed single-exponential kinetics. Experimental data are shown for the overall and initial (insert) oxidative half reaction catalyzed by wild type OYE1 (gray) and cpOYE303 (black). Curve fits are displayed as red lines.

(relative to 578 nm for wild type OYE1) reflect changes in the FMN redox potential of ~20 mV which suggest small conformational and environmental perturbations near the cofactor. Nevertheless, the change in redox potentials for the cpOYE variants did not show a clear correlation with catalytic activity for our three substrates.

CONCLUSIONS

We have identified a series of circularly permuted OYE variants with enhanced ene-reductase activity for two representative enones and an enal. For all three substrates, the new protein termini of catalytically active and improved enzymes fall into the same four structural regions including three loops and a helical subdomain near the active site. The functional benefits of new termini in these regions varied with substrate, presumably reflecting subtle differences in protein structure and interactions with the substrates. The native enzyme's high enantioselectivity was preserved in all cpOYE variants, and catalytic activity for **1** and (*S*)-**5** was improved by >10-fold. The rapid reaction kinetics analysis of the oxidative and reductive half reactions in wild type OYE1 and cpOYE303 suggests that the functional gains can almost exclusively be attributed to improvements of the rate-limiting oxidative half reaction with **1**. Further in-depth studies of the individual steps in the reaction cycle will be required to explore whether the observed rate enhancements are more specifically due to changes in binding of **1**, release of (*R*)-**2**, or the catalytic step. Initial evidence in support of beneficial changes to substrate/product affinity upon CP was found in the absence of the characteristic charge-transfer complex (E·FMN_{ox}·NADPH) in the reductive half reaction of cpOYE303. The accumulation of the complex in wild type OYE1 has been associated with a required conformational change involving loop 5, the same loop where the new protein termini in cpOYE303 are located. The increased conformational flexibility of a protein's termini region is well established in the literature and could explain the improved catalytic activity in our engineered OYE variants. Crystallographic and in-depth biophysical studies will help to further rationalize the observed differences in catalytic performance. Beyond the exploration of fundamental aspects of enzyme catalysis, our results demonstrate that CP offers an effective strategy for improving the catalytic performance of OYE1. Although a direct comparison with other mutagenesis-based engineering approaches is complicated by differences in reaction conditions and substrates, the rate enhancements for our cpOYE variants are of similar magnitude or better than for previously reported OYE variants.[22,53] For future experiments, the structural and functional similarities among enzymes of the OYE family suggest that CP could result in similar functional gains in other family members. Furthermore, selected cpOYE variants do not necessarily mark the end point of a protein engineering project but can serve as novel templates for subsequent mutagenesis experiments, allowing for even greater diversity in tailoring these biocatalysts to specific conditions and substrates. On the technical side, the use of a chemically defined cpOYE gene library in combination with the PURE system dramatically accelerated the process of identifying catalytically improved cpOYE variants for any substrate of choice. As technological advances continue to raise efficacy and lower costs, we envision such synthetic protein engineering approaches to become a popular new tool for synthetic biologists. For engineering OYE and cofactor-dependent enzymes in general, the use of IVTT systems also offers unprecedented opportunities for combinatorial approaches to exploring the functional impact of cofactor substitutions.

dx.doi.org/10.1021/ja4074886 | J. Am. Chem. Soc. 2013, 135, 14425−14432

■ ASSOCIATED CONTENT

Supporting Information

Michealis–Menten kinetics, absorbance spectra, validation of in vitro transcription/translation systems, and percent conversion of ketoisophorone by wild-type OYE1. This material is available free of charge via the Internet at http://pubs.acs.org.

■ AUTHOR INFORMATION

Corresponding Author

sal2@emory.edu

Notes

The authors declare no competing financial interest.

■ ACKNOWLEDGMENTS

The authors thank Drs. Roberto Orru and Dale Edmondson for their assistance with the stopped flow experiments and members of the Atlanta Flavin Group and the Lutz lab for helpful comments and suggestions. Support with PURExpress by Corinna Tuckey from New England Biolabs (Ipswich, MA) is acknowledged. This work was in part funded by the U.S. National Science Foundation (Grants CBET 0730312 and 1159434).

■ REFERENCES

(1) Lu, S. M.; Bolm, C. *Chemistry* **2008**, *14*, 7513.
(2) Taylor, C. J. S. N.; Jaekel, C. *Adv. Synth. Catal.* **2008**, *350*, 2708.
(3) Martin, N. J. A.; List, B. *J. Am. Chem. Soc.* **2006**, *128*, 13368.
(4) Tuttle, J. B.; Ouellet, S. G.; MacMillan, D. W. C. *J. Am. Chem. Soc.* **2006**, *128*, 12662.
(5) Bornscheuer, U. T.; Huisman, G. W.; Kazlauskas, R. J.; Lutz, S.; Moore, J. C.; Robins, K. *Nature* **2012**, *485*, 185.
(6) Nestl, B. M.; Nebel, B. A.; Hauer, B. *Curr. Opin. Chem. Biol.* **2011**, *15*, 187.
(7) Wohlgemuth, R. *Curr. Opin. Biotechnol.* **2010**, *21*, 713.
(8) Kawai, Y.; Inaba, Y.; Tokitoh, N. *Tetrahedron: Asymmetry* **2001**, *12*, 309.
(9) Kosjek, B.; Fleitz, F. J.; Dormer, P. G.; Kuethe, J. T.; Devine, P. N. *Tetrahedron: Asymmetry* **2008**, *19*, 1403.
(10) Hall, M.; Stueckler, C.; Hauer, B.; Stuermer, R.; Friedrich, T.; Breuer, M.; Kroutil, W.; Faber, K. *Eur. J. Org. Chem.* **2008**, *9*, 1511.
(11) Swiderska, M. A.; Stewart, J. D. *J. Mol. Catal. B: Enzym.* **2006**, *42*, 52.
(12) Adalbjornsson, B. V.; Toogood, H. S.; Fryszkowska, A.; Pudney, C. R.; Jowitt, T. A.; Leys, D.; Scrutton, N. S. *ChemBioChem* **2010**, *11*, 197.
(13) Toogood, H. S.; Fryszkowska, A.; Hare, V.; Fisher, K.; Roujeinikova, A.; Leys, D.; Gardiner, J. M.; Stephens, G. M.; Scrutton, N. S. *Adv. Synth. Catal.* **2008**, *350*, 2789.
(14) Toogood, H. S.; Gardiner, J. M.; Scrutton, N. S. *ChemCatChem* **2010**, *2*, 892.
(15) Stueckler, C.; Mueller, N. J.; Winkler, C. K.; Glueck, S. M.; Gruber, K.; Steinkellner, G.; Faber, K. *Dalton Trans.* **2010**, *39*, 8472.
(16) Hall, M.; Stueckler, C.; Ehammer, H.; Pointner, E.; Oberdorfer, G.; Gruber, K.; Hauer, B.; Stuermer, R.; Kroutil, W.; Macheroux, P.; Faber, K. *Adv. Synth. Catal.* **2008**, *350*, 411.
(17) Winkler, C. K.; Tasnadi, G.; Clay, D.; Hall, M.; Faber, K. *J. Biotechnol.* **2012**, *162*, 381.
(18) Schittmayer, M.; Glieder, A.; Uhl, M. K.; Winkler, A.; Zach, S.; Schrittwieser, J. H.; Kroutil, W.; Macheroux, P.; Gruber, K.; Kambourakis, S.; Rozzell, J. D.; Winkler, M. *Adv. Synth. Catal.* **2011**, *353*, 268.
(19) Pompeu, Y. A.; Sullivan, B.; Walton, A. Z.; Stewart, J. D. *Adv. Synth. Catal.* **2012**, *354*, 1949.
(20) Hulley, M. E.; Toogood, H. S.; Fryszkowska, A.; Mansell, D.; Stephens, G. M.; Gardiner, J. M.; Scrutton, N. S. *ChemBioChem* **2010**, *11*, 2433.
(21) Toogood, H. S.; Fryszkowska, A.; Hulley, M.; Sakuma, M.; Mansell, D.; Stephens, G. M.; Gardiner, J. M.; Scrutton, N. S. *ChemBioChem* **2011**, *12*, 738.
(22) Bougioukou, D. J.; Kille, S.; Taglieber, A.; Reetz, M. T. *Adv. Synth. Catal.* **2009**, *351*, 3287.
(23) Padhi, S. K.; Bougioukou, D. J.; Stewart, J. D. *J. Am. Chem. Soc.* **2009**, *131*, 3271.
(24) Hall, M.; Bommarius, A. S. *Chem. Rev.* **2011**, *111*, 4088.
(25) Reich, S.; Hoeffken, H. W.; Rosche, B.; Nestl, B. M.; Hauer, B. *ChemBioChem* **2012**, *13*, 2400.
(26) Brown, B. J.; Hyun, J. W.; Duvvuri, S.; Karplus, P. A.; Massey, V. *J. Biol. Chem.* **2002**, *277*, 2138.
(27) Vaz, A. D. N.; Chakraborty, S.; Massey, V. *Biochemistry* **1995**, *34*, 4246.
(28) Niino, Y. S.; Chakraborty, S.; Brown, B. J.; Massey, V. *J. Biol. Chem.* **1995**, *270*, 1983.
(29) Massey, V.; Schopfer, L. M. *J. Biol. Chem.* **1986**, *261*, 1215.
(30) Fox, K. M.; Karplus, P. A. *Structure* **1994**, *2*, 1089.
(31) Karplus, P. A.; Fox, K. M.; Massey, V. *FASEB J.* **1995**, *9*, 1518.
(32) Yu, Y.; Lutz, S. *Trends Biotechnol.* **2011**, *29*, 18.
(33) Qian, Z.; Lutz, S. *J. Am. Chem. Soc.* **2005**, *127*, 13466.
(34) Qian, Z.; Fields, C. J.; Lutz, S. *ChemBioChem* **2007**, *8*, 1989.
(35) Qian, Z.; Horton, J. R.; Cheng, X.; Lutz, S. *J. Mol. Biol.* **2009**, *393*, 191.
(36) Whitehead, T. A.; Bergeron, L. M.; Clark, D. S. *Protein Eng. Des. Sel.* **2009**, *22*, 607.
(37) Stephen, P.; Tseng, K. L.; Liu, Y. N.; Lyu, P. C. *Chem. Commun. (Cambridge, U. K.)* **2012**, *48*, 2612.
(38) Guntas, G.; Kanwar, M.; Ostermeier, M. *PLoS One* **2012**, *7*, e35998.
(39) Ueda, T.; Shimizu, Y.; Inoue, A.; Tomari, Y.; Suzuki, T.; Yokogawa, T.; Nishikawa, K. *Nat. Biotechnol.* **2001**, *19*, 751.
(40) Protein Generation Using a Reconstituted System. In *Protein Engineering Handbook*; Ying, B. W., Ueda, T., Eds.; Wiley-VCH: Weinheim, Germany, 2009; Vol. 2.
(41) Brown, B. J.; Deng, Z.; Karplus, P. A.; Massey, V. *J. Biol. Chem.* **1998**, *273*, 32753.
(42) Reitinger, S.; Yu, Y.; Wicki, J.; Ludwiczek, M.; D'Angelo, I.; Baturin, S.; Okon, M.; Strynadka, N. C.; Lutz, S.; Withers, S. G.; McIntosh, L. P. *Biochemistry* **2010**, *49*, 2464.
(43) Abramovitz, A. S.; Massey, V. *J. Biol. Chem.* **1976**, *251*, 5327.
(44) Stuermer, R.; Hauer, B.; Hall, M.; Faber, K. *Curr. Opin. Chem. Biol.* **2007**, *11*, 203.
(45) Wada, M.; Yoshizumi, A.; Noda, Y.; Kataoka, M.; Shimizu, S.; Takagi, H.; Nakamori, S. *Appl. Environ. Microbiol.* **2003**, *69*, 933.
(46) Kataoka, M.; Kotaka, A.; Hasegawa, A.; Wada, M.; Yoshizumi, A.; Nakamori, S.; Shimizu, S. *Biosci., Biotechnol., Biochem.* **2002**, *66*, 2651.
(47) Fryszkowska, A.; Toogood, H.; Sakuma, M.; Gardiner, J. M.; Stephens, G. M.; Scrutton, N. S. *Adv. Synth. Catal.* **2009**, *351*, 2976.
(48) Ay, J.; Hahn, M.; Decanniere, K.; Piotukh, K.; Borriss, R.; Heinemann, U. *Proteins* **1998**, *30*, 155.
(49) Chu, V.; Freitag, S.; Le Trong, I.; Stenkamp, R. E.; Stayton, P. S. *Protein Sci.* **1998**, *7*, 848.
(50) Manjasetty, B. A.; Hennecke, J.; Glockshuber, R.; Heinemann, U. *Acta Crystallogr., Sect. D: Biol. Crystallogr.* **2004**, *60*, 304.
(51) Pieper, U.; Hayakawa, K.; Li, Z.; Herzberg, O. *Biochemistry* **1997**, *36*, 8767.
(52) Matthews, R. G.; Massey, V.; Sweeley, C. C. *J. Biol. Chem.* **1975**, *250*, 9294.
(53) van den Heuvel, R. H.; van den Berg, W. A.; Rovida, S.; van Berkel, W. J. *J. Biol. Chem.* **2004**, *279*, 33492.